Particle Morphology Effects on Flow Characteristics of PS304 Plasma Spray Coating Feedstock Powder Blend

Malcolm K. Stanford
University of Dayton, Dayton, Ohio

Christopher DellaCorte
Glenn Research Center, Cleveland, Ohio

Daniel Eylon
University of Dayton, Dayton, Ohio

Since its founding, NASA has been dedicated to the advancement of aeronautics and space science. The NASA Scientific and Technical Information (STI) Program Office plays a key part in helping NASA maintain this important role.

The NASA STI Program Office is operated by Langley Research Center, the Lead Center for NASA's scientific and technical information. The NASA STI Program Office provides access to the NASA STI Database, the largest collection of aeronautical and space science STI in the world. The Program Office is also NASA's institutional mechanism for disseminating the results of its research and development activities. These results are published by NASA in the NASA STI Report Series, which includes the following report types:

- TECHNICAL PUBLICATION. Reports of completed research or a major significant phase of research that present the results of NASA programs and include extensive data or theoretical analysis. Includes compilations of significant scientific and technical data and information deemed to be of continuing reference value. NASA's counterpart of peer-reviewed formal professional papers but has less stringent limitations on manuscript length and extent of graphic presentations.

- TECHNICAL MEMORANDUM. Scientific and technical findings that are preliminary or of specialized interest, e.g., quick release reports, working papers, and bibliographies that contain minimal annotation. Does not contain extensive analysis.

- CONTRACTOR REPORT. Scientific and technical findings by NASA-sponsored contractors and grantees.

- CONFERENCE PUBLICATION. Collected papers from scientific and technical conferences, symposia, seminars, or other meetings sponsored or cosponsored by NASA.

- SPECIAL PUBLICATION. Scientific, technical, or historical information from NASA programs, projects, and missions, often concerned with subjects having substantial public interest.

- TECHNICAL TRANSLATION. English-language translations of foreign scientific and technical material pertinent to NASA's mission.

Specialized services that complement the STI Program Office's diverse offerings include creating custom thesauri, building customized data bases, organizing and publishing research results . . . even providing videos.

For more information about the NASA STI Program Office, see the following:

- Access the NASA STI Program Home Page at *http://www.sti.nasa.gov*

- E-mail your question via the Internet to help@sti.nasa.gov

- Fax your question to the NASA Access Help Desk at 301–621–0134

- Telephone the NASA Access Help Desk at 301–621–0390

- Write to:
  NASA Access Help Desk
  NASA Center for AeroSpace Information
  7121 Standard Drive
  Hanover, MD 21076
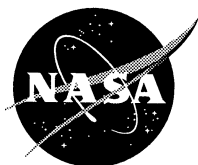
Particle Morphology Effects on Flow Characteristics of PS304 Plasma Spray Coating Feedstock Powder Blend

Malcolm K. Stanford
University of Dayton, Dayton, Ohio

Christopher DellaCorte
Glenn Research Center, Cleveland, Ohio

Daniel Eylon
University of Dayton, Dayton, Ohio

Acknowledgments

PARTICLE MORPHOLOGY EFFECTS ON FLOW CHARACTERISTICS OF PS304 PLASMA SPRAY COATING FEEDSTOCK POWDER BLEND

Malcolm K. Stanford
University of Dayton
Dayton, Ohio 45469–0121

Christopher DellaCorte
National Aeronautics and Space Administration
Glenn Research Center
Cleveland, Ohio 44135

Daniel Eylon
University of Dayton
Dayton, Ohio 45469–0240

Abstract

The effects of BaF_2-CaF_2 particle morphology on PS304 feedstock powder flow ability have been investigated. BaF_2-CaF_2 eutectic powders were fabricated by comminution (*angular*) and by gas atomization (*spherical*). The fluoride powders were added incrementally to the other powder constituents of the PS304 feedstock: nichrome, chromia, and silver powders. A linear relationship between flow time and concentration of BaF_2-CaF_2 powder was found. Flow of the powder blend with spherical BaF_2-CaF_2 was better than the angular BaF_2-CaF_2. Flow ability of the powder blend with *angular* fluorides decreased linearly with increasing fluoride concentration. Flow of the powder blend with *spherical* fluorides was independent of fluoride concentration. Results suggest that for this material blend, particle morphology plays a significant role in powder blend flow behavior, offering potential methods to improve powder flow ability and enhance the commercial potential. These findings may have applicability to other difficult-to-flow powders such as cohesive ceramics.

Introduction

The eutectic composition of barium fluoride and calcium fluoride ($70BaF_2$-$30CaF_2$) is a solid lubricant in PS304, a plasma spray deposited composite solid lubricant coating for friction and wear reduction in turbomachinery applications (refs. 1 to 6). PS304 coating is made from a powder blend consisting of nichrome, chromia, silver, and eutectic barium fluoride—calcium fluoride powders. Experience with the blended powder feedstock for this coating indicates that the particle size of the fluoride constituent has a significant effect on the flow ability of the PS304 powder blend. This investigation studied eutectic BaF_2-CaF_2 powders with different morphologies from two powder fabrication techniques, *comminution* and *gas atomization*. The objective of this study was to establish the role of eutectic particle morphology in PS304 powder blend flow ability in order to improve feedstock properties and enhance the commercial potential. The fabrication techniques in this study are limited to production of primary particles and exclude spray-dried agglomerates. Previous research has shown that spray-dried particles can have flow problems associated with particle surface roughness (ref. 7). Particle porosity and the addition of a binder in agglomerates may also have an adverse effect on the performance of the coating system in service. The data generated by this study are unique to the PS304 powder blend, but the results are expected to have a broader application to other classes of composite powder blends.

Background

The PS304 plasma spray coating was developed at NASA Glenn Research Center (ref. 8) for the reduction of sliding friction and wear in turbomachinery applications at temperatures from subambient up to 650 °C. The composition of this coating is 60 wt% nichrome (80Ni-20Cr), 20 wt% chromia (Cr_2O_3), 10 wt% silver, and 10 wt% eutectic BaF_2-CaF_2. Nichrome serves as a binder and provides wear resistance and Cr_2O_3 is for wear resistance. Silver and BaF_2-CaF_2 are solid lubricants at low temperature and high temperature, respectively.

The plasma spray process propels particles of the deposition material through a plasma flame produced by the ionization of an inert gas (ref. 9). The plasma heats the particles above their melting temperature. Molten particles then impact the substrate, where they quickly solidify. The buildup of subsequent particles adds thickness to the developing coating. The feedstock is typically a powder to facilitate control of the rapid melting and resolidification of the coating material. Where multicomponent coating systems are to be deposited, the feedstock can be a powder blend of the coating constituents.

In a preliminary study it was found that feedstock powder for PS304 would intermittently clog in the plasma spray feed hopper, related to the presence of the BaF_2-CaF_2 particles (ref. 10). When BaF_2-CaF_2 particles were under 50 μm, feedstock had poor flow characteristics and clogged in the feed hopper.

Calcium fluoride and barium fluoride may be mined or synthesized by wet chemistry. The largest deposits of calcium fluoride are in China, Mexico, and South Africa (ref. 11). The bulk of these are used for steel flux, production of aluminum, and production of hydrofluoric acid. High-purity fluorides are used for optics and for high-temperature lubricants. They are typically produced by wet chemistry due to the cost involved in removing impurities from mined materials. The material is precipitated from a calcium or barium-rich solution with fluorine gas. This process yields very fine fluoride particles (~1 μm) that are extremely difficult to transfer using standard bins and hoppers due to their high surface area, which makes the particles tend to agglomerate. To improve powder handling, the precipitated product may be fused and subsequently produced in a size that is more easily processed. To fabricate BaF_2-CaF_2 powders, the two constituents must be fused and the bulk material is converted to a powder.

Conventional fabrication of ceramic powder can be achieved with a number of comminution processes. Unfortunately, these processes yield particles that are irregular and angular in shape, with poor flow characteristics compared to smoother, more rounded particles (ref. 12). Both the size and the shape of the powder particles are believed to affect the flow ability of the powder blends. This study examines the effect of fluoride shape on the flow characteristics of PS304 feedstock powder.

Powder Flow and Powder Fabrication

As particles in a powder system get smaller, they have greater tendency to adhere to one another rather than to fall away under the influence of gravity (ref. 13). This is due to the fact that the surface area of the particles becomes large in proportion to their mass. Therefore, the surface forces of friction and cohesion begin to dominate gravitational forces as particle size decreases. Increasing interparticle friction and cohesion reduces the flow ability of the powder.

Particle shape also affects the flow characteristics of powders (ref. 12). As a particle departs from a low energy geometry such as a sphere, the ratio of its surface area to volume increases. Depending on the fabrication method, particles can take on many different shapes including spherical, rounded, and angular.

The flow ability of a powder can be quantified by measuring its gravity-driven flow rate through a calibrated orifice. The conventional method measures the time required for a 50-g sample to flow through a standardized funnel (ref. 14). Grey and Beddow (ref. 15) studied the flow characteristics of copper powders with spherical, irregular, and flake morphologies and showed that as the shape became less spherical, the flow properties were degraded. Little work has been published on the flow characteristics of spherical ceramic powders because ceramics, owing to their generally high melting temperatures, are typically angular fabricated by traditional comminution processes.

The level of interparticle friction in a powder can be estimated with the *apparent density*, which is the bulk density as poured and without agitation (ref. 12). As interparticle friction increases, apparent density decreases.

Comminution (crushing) processes reduce the size of a material by the application of a combination of compressive and shear forces (ref. 16). These processes take advantage of the naturally occurring defects in ceramic materials, such as grain boundaries, pores and microcracks, as well as the inherent brittleness (ref. 17).

The dependence of the fracture strength of a brittle particle on a preexisting flaw is described by the well-known Griffith relationship (ref. 18). It states that fracture strength σ_f of a material is inversely proportional to the square root of the flaw size c:

$$\sigma_f = \sqrt{\frac{2\gamma_f \cdot E}{\pi\, c}}$$

where E is the material's modulus of elasticity and γ_f is the energy required to create two new fracture surfaces. When the stress on a particle due to comminution is greater than σ_f, fracture and size reduction will take place. Due to their brittle nature, the powders will be angular.

Comminution can be a very inefficient and energy-intensive process despite the brittle nature of ceramics (ref. 19). This is especially the case in the production of fine powders where with each particle fragmentation, flaw population and size decrease. When there are fewer and smaller flaws, comminution energy tends to go toward particle deformation and heat generation.

All commercial applications of PS304 to date have used fluorides produced by comminution. For this study, a development project was implemented to also produce *spherical* fluorides. The high energy required to melt ceramics typically makes fusion-based processes undesirable. However, the melting temperatures of fluorides are relatively low due to their highly ionic bonding character (refs. 20 and 21). As shown in figure 1, CaF_2 melts at 1410 °C and BaF_2 melts at 1338 °C (ref. 22). Furthermore, at of 70 wt% BaF_2 and 30 wt% CaF_2, a eutectic is formed that melts just below 1050 °C. This composition was selected for the current application due to the ease of processing afforded by the reduced melting point, which also enabled the use of gas atomization for fabrication of novel spherical BaF_2-CaF_2 particles.

The principle elements of a gas atomization process are shown schematically in figure 2 (refs. 23 and 24). Molten material is contained in a tundish, which has a nozzle with an inner diameter D. The difference between the processing temperature and the melting point of the material is the superheat, which prevents the material from freezing prematurely. The molten material is allowed to flow through the nozzle under the influence of gravity. As the liquid stream exits the nozzle, the pressure drop created by the flow of the atomizing fluid and the impact of the gas stream causes the stream to disperse. The surface tension of the molten material encourages the formation of rounded or spherical droplets (ref. 25). The droplets then cool and solidify forming particles as they fall to a collection tank at a distance H below the nozzle.

Experimental Procedure

Nichrome particles (fig. 3(a)) are 44 to 74 µm in size (table I) and have a rounded shape resulting from water atomization (refs. 23 and 24). Chromia particles (fig. 3(b)) are 30 to 44 µm in size (table I) and have an angular morphology. This powder was fabricated by sintering the bulk material into large bricks and then comminuting the bricks into a powder. The spherical silver particles (fig. 3(c)), fabricated by gas atomization, are 45 to 100 µm in diameter. The sizes and shapes of the nichrome, chromia, and silver powders were available as commercial products and were not modified in this study.

To produce the BaF_2-CaF_2 eutectic, shown in figure 3(d), 70 wt% BaF_2 and 30 wt% CaF_2 were combined in a graphite crucible and melted under vacuum at 1100 °C followed by vacuum cooling. The solidified material was then removed from the crucible for powder fabrication by the two methods.

In the first stage of size reduction of the angular powder, large chunks of the fused fluoride material were fed into a jaw crusher that compresses the material between two opposing and inclined surfaces. One surface is fixed and the other reciprocates, providing the crushing force. Once the material is small enough to fit through the gap at the bottom of the two crushing surfaces, it is collected in a bin. This size-reduction step produces a coarse powder similar to fine gravel.

To further reduce the angular fluoride powder size, the powder retrieved from the jaw crusher was then fed into a disk mill. A disk mill feeds the powder between two opposing disk surfaces. One disk is stationary while the other rotates. The disks have teeth that run along their radii to fracture the particles trapped between them. The teeth allow less space for the particles as they reach the outer edge of the disks such that the minimum gap determines the largest particle that will fall between the disks.

Atomization of the fluorides was performed with a commercially available small-scale close-coupled gas atomization system (ref. 26). Approximately 1400 g of 150-μm fluoride eutectic powder was obtained for atomization. The feedstock was induction-melted under an argon cover in a high-purity graphite crucible at 200 °C superheat. The crucible also acted as the susceptor for the induction power. The melt was bottom-tapped from the crucible directly into the atomization nozzle. Commercial purity argon was used for the atomization gas and a secondary quench of deionized water was used to cool and confine the nascent powder. Powder was retrieved from the quenching medium by settling and decanting. The concentrated powder was then washed in acetone, decanted and dried at a low temperature (below 100 °C). About 99 percent of the crucible charge was recovered as powder.

The fluoride powders were classified by screening according to ASTM standard specification B 214–99. This procedure was performed using screens manufactured according to ASTM standard specification E–11. The screens were stacked vertically in order of coarsest mesh to finest mesh. The screen mesh sizes used were numbers 140, 170, 200, 230, 270, and 325. The screening instrument uses a vertically oscillating column of air and a combination of vertical and horizontal tappers to separate the particles according to size (table I).

The flow rate of each powder blend was measured twice according to ASTM B 213–97. For this measurement, a 50-g sample of the powder blend being tested was loaded into a Hall flowmeter. A schematic of the apparatus is shown in figure 4. The Hall flowmeter was found to be a reliable indicator of the flow ability powder blends through the powder feed system for the studied plasma spray system. Powders that consistently flowed through the plasma spray powder feed system also flowed through the Hall flowmeter. Conversely, powders that did not flow through the plasma spray equipment did not flow through the flowmeter. The Hall flowmeter has been used in recent studies to characterize the flow rate of plasma spray feedstock powders (refs. 7 and 27).

For each flow test, a powder blend consisting of 60-g nichrome, 20-g chromia, 10-g silver, and an incrementally increasing amount of either angular or spherical fluoride powder was prepared by mixing the constituents together in a 125-mL high-density polyethylene bottle until the powder was well blended. A 50-g sample was obtained from this powder blend for flow testing. A 0.01-s precision digital stopwatch was used to measure the time it took the entire 50-g sample to exit the funnel, recorded to the nearest 0.1 s, which was designated the *flow time*. The amount of fluoride powder used in the blend was then increased by 1.0 g and the test was repeated. This procedure was repeated from 0 wt% up to 10 wt% fluoride. Data were reported on a plot of flow time versus the weight percent of fluoride in the powder blend. Tests were performed at room temperature and 50 percent relative humidity.

Results and Discussion

Figure 5 shows photomicrographs of the angular and spherical fluoride powders. The particles collected from the jaw crusher were smaller than 2 mm. The particles collected from the disk mill were smaller than 200 μm. The crushed and ground fluoride particles had an angular shape. The surfaces of these particles had fracture patterns consistent with brittle fracture.

The particles produced by atomization had a spherical shape. The surfaces of the particles showed equiaxed grains, which is characteristic of a material that has undergone rapid solidification (ref. 12). The surfaces of the particles were generally smooth, with a few attached satellites from smaller particles that collided with the larger ones before they were completely solidified. The particle diameters had a log-normal distribution that ranged from 0.82 to 124 μm, as determined by the light blockage particle size analysis technique (ref. 28). The median particle diameter was approximately 17 μm. This particle size distribution was finer than expected based on the previous experience of the powder manufacturer.

The weight percentages of the crushed and ground fluoride powder collected per screening run are shown in figure 6(a). The remaining powder was collected on the pan beneath the number 325 sieve. Due to their aspect ratio, some particles were able to fit through the screens by their smallest dimension. Since screening was used to classify the powders, the surface to volume ratio of the angular fluorides was nearly the same as that of the spherical fluorides. Therefore, the observed effect of particle morphology on flow ability will be separate from the effect of the ratio of surface area to volume.

The atomized fluoride powder weight percentages collected per screening run are shown in figure 6(b). The remaining powder was collected on the pan beneath the number 325 sieve.

An equal particle size distribution by mass of −140 + 325 mesh (45 to 106 μm) powders was prepared of comminuted and of atomized fluorides (table I). The fluoride powders were added incrementally to a powder blend consisting of 60-g nichrome, 20-g chromia, and 10-g silver. A 50-g sample of this blend was then used in the flow test. The reported flow time is the average value from two consecutive tests. The results are shown graphically in figure 7.

The flow times of the powder with the *spherical* fluorides were always lower than the *angular* fluorides. The relationship between flow time of the powder blend with respect to increasing fluoride content was linear over the range from 0 to 10 wt%. The variability in the flow time measurement at each weight percentage of fluoride, based on 2 runs per test condition, was typically less than 0.5 percent. Variability with angular fluorides was slightly higher than with spherical fluorides. Error bars are not shown on the plot (fig. 7) because they do not span the width of the data labels. The flow times of the powder blend using the angular powder fit a line described by $y = 0.5094x + 26.303$, where y and x represent flow time and fluoride concentration, respectively. The correlation coefficient was $R^2 = 0.9896$. The flow times of the powder blend with the spherical powder fit a line described by $y = -0.003636x + 26.41$. The correlation coefficient was $R^2 = 0.0068$, indicating that there was essentially no relationship between fluoride concentration and flow time. The slope of the line indicates the effect of the fluoride powder concentration on the flow ability of the powder, the lower the slope, the lower the effect. The intercept of the line approximates the flow time at 0 wt% fluoride. By statistical hypothesis testing, the intercepts of both lines could not be distinguished from the measured value (26.3 s). In addition, the slope of the line representing the blend with spherical fluorides was impossible to differentiate from zero.

Based on the rule of mixtures, the volume of a standard 50-g powder sample of PS304 feedstock powder is expected to increase with increasing fluoride content because the theoretical density of the fluoride, 4.01 g/cm^3, is less than the other constituents. Nichrome, chromia, and silver are 8.57, 5.22, and 10.49 g/cm^3, respectively (table I). If the flow time of the powder blend were only dependent upon the volume of powder transferred though the funnel with no particle interaction effects, the flow time of a 50-g sample with 10 wt% fluoride would be expected to take 9 percent longer than a 50-g sample with no fluorides, due to the 9 percent increased volume for the 50-g sample. The calculated flow times based only on increased volume are shown in figure 7. The powder blend with 10 wt% *angular* fluorides would then have a flow time of about 29 s as shown by the calculated line in figure 7, instead of the measured 31.6 s, if volume alone was considered. Based on this, the measured flow time using angular fluorides was approximately 9 percent higher than expected. This difference is thought to be due to the increased interparticle friction and its resulting increase on the void fraction in the powder blend. Using *spherical* fluorides, the flow time was independent of the fluoride concentration. In this case, the effects of interparticle friction and reduction of powder density were offset by the improvement in flow given by the spherical fluorides.

To confirm the increase in volume with fluoride concentration, the *apparent density* of the powders were measured at 0 and 10 wt% fluoride. The apparent density of the PS304 powder with 10 wt% of either fluoride type was nearly 5 percent lower than that for the powder blend containing only nichrome, chromia, and silver. This measurement is the reciprocal specific volume and accounts for the interparticle friction that is present in the powder blend both before and after the fluoride constituent was added. Clearly, the increase in the flow time after the addition of the fluorides is proportional to the decrease in apparent density of the powder blend. However, the decreased density alone does not fully account for the increased flow time.

A probable explanation for the difference in flow characteristics is the particle morphology. Irregularly shaped particles have relatively poor flow characteristics due to higher surface area, which results in higher interparticle friction (ref. 12). The flat surfaces of the *angular* fluoride particles tend to provide much greater effective contact area with adjacent particles. On the other hand, *spherical* fluorides are most likely to have point contact with other particles; therefore, *angular* fluorides are expected to have higher interparticle friction. In addition, irregular shape makes interaction with adjacent particles more random than the more regularly shaped spherical particles, which might explain the slightly higher variability observed in the measurements for the flow times of the powder blends containing angular fluorides. Furthermore, the spherical fluorides are more able to roll against the other powder constituents. Since rolling friction is typically lower than sliding friction, the powder blends with angular fluorides would tend to have higher interparticle friction. In every case studied, the spherical fluoride powders offered flow properties significantly better than the angular fluorides, which appears to be closely linked to the effect of particle morphology on interparticle friction.

Summary and Conclusions

The objective of this investigation was to identify the effects of BaF$_2$-CaF$_2$ powder particle morphology on the flow characteristics of PS304 feedstock. Based on the results of this study, the following conclusions are made:
1. Fluoride particle morphology has a significant effect on powder flow. Improved PS304 powder blend flow properties can be obtained using *spherical* fluoride powder in place of the *angular* fluoride currently used.
2. Increased flow time for powder blends containing *angular* fluorides was linearly proportional to the fluoride weight percent in the 0 to 10 wt% fluoride range.

3. Argon gas atomization of eutectic BaF_2-CaF_2 can be successfully used to fabricate spherical powder. Based on these findings, there may be other relatively low melting point engineering ceramics that could be fabricated by gas atomization. This would be of great benefit to processes that presently rely on angular, ceramic powders that tend to be subject to the effects of interparticle cohesion and friction.

4. The flow times of the PS304 feedstock with *spherical* fluorides are essentially independent of fluoride concentration. This finding is underscored by the fact that the increase in flow time with increased fluoride concentration predicted by the rule of mixtures is not observed for spherical fluorides. This behavior is related to the morphology of the fluoride particles.

5. The results presented specifically concern the PS304 solid lubricant powder blend. However, the generalized findings regarding powder fabrication and the effect of morphology on interparticle friction-controlled powder blend phenomena may offer insight into the behavior of other powder blend systems.

References

1. DellaCorte, C., et al.: Performance and Durability of High Temperature Foil Air Bearings for Oil-Free Turbomachinery. *Tribology Transactions*, vol. 43, no. 4, 2000, pp. 744–780.

2. DellaCorte, C.; and Wood, J.C.: High Temperature Solid Lubricant Materials for Heavy Duty and Advanced Heat Engines. NASA TM–106570, 1994.

3. Laskowski, J.A.; and DellaCorte, C.: Friction and Wear Characteristics of Candidate Foil Bearing Materials From 25 °C to 800 °C. *Lubrication Engineering*, vol. 52, 1996, pp. 605–612.

4. DellaCorte, C.; and Edmonds, B.J.: Preliminary Evaluation of PS300: A New Self-Lubricating High Temperature Composite Coating for Use to 800 °C. NASA TM–107056, 1996.

5. DellaCorte, C.: The Evaluation of a Modified Chrome Oxide Based High Temperature Solid Lubricant Coating for Foil Gas Bearings. NASA/TM—1998-208660, 1998. http://gltrs.grc.nasa.gov/GLTRS Accessed.

6. DellaCorte, C.: Evaluation of Advanced Solid Lubricant Coatings For Foil Air Bearings Operating at 25 and 500 °C. NASA/TM—1998-206619, 1998. http://gltrs.grc.nasa.gov/GLTRS Accessed.

7. Kim, B.K.; Lee, D.W.; and Ha, G.H.: Plasma Spray Coating of Spray-Dried Cr_2O_3/3 wt% TiO2 Powder. *Journal of Thermal Spray Technology*, vol. 10, no. 1, 2001, pp. 133–137.

8. DellaCorte, C.; and Edmonds, B.J.: U.S. Patent 5,866,518, 1999.

9. Ingham, H.S.; and Shepard, A.P.: Flame Spray Handbook. Metco, New York, Metco, 1965.

10. DellaCorte, C.; and Edmonds, B.J.: Unpublished report, 1999.

11. McClurg, G.B.: Fluorspar. *The American Ceramic Society Bulletin*, vol. 76, no. 6, pp. 99–101, 1997.

12. German, R.M.: *Powder Metallurgy Science*. Metal Powder Industries Federation, Princeton, 1984.

13. Zimon, A.D.: *Adhesion of Dust and Powder*. Second ed., Consultants Bureau, New York, 1982.

14. Standard Test Method for Flow Rate of Metal Powders. Annual Book of ASTM Standards. ASTM B 213–97, vol. 02.05. American Society for the Testing of Materials, West Conshohocken, PA, 1998.

15. Grey, R.O.; and Beddow, J.K.: On the Hausner Ratio and Its Relationship to Some Properties of Metal Powders. *Powder Technology*, vol. 2, 1969, pp. 323–326.

16. Tanaka, T.; and Kanda, Y.: Crushing and Grinding. In *Powder Technology Handbook*, Second ed., Marcel Dekker, Inc., New York, 1997.

17. Reed, J.S.: *Introduction to the Principles of Ceramic Processing*. John Wiley & Sons, New York, 1988.

18. Griffith, A.A.: The Phenomena of Rupture and Flow in Solids. *Philosophical Transactions of the Royal Society of London, Series A* 221, pp. 163–168.

19. Malghan, S.G.: Communition. In *Engineered Materials Handbook*, vol. 4, Ceramics and Glasses, ASM International, Materials Park, OH, 1991.

20. Richerson, D.W.: *Modern Ceramic Engineering: Properties, Processing, and Use in Design*. Marcel Dekker, Inc., New York, 1992.

21. Pauling, L.: *The Nature of the Chemical Bond and the Structure of Molecules and Crystals: An Introduction to Modern Structural Chemistry*. Third ed., Cornell University Press, Ithaca, NY, 1960.

22. Rolin, M.; and Clausier, M.: *Revue Internationale des Hautes Températures et des Réfractaires: Bulletin de la Société Nationale Française des Hautes Temperatures et des Réfractaires*. 4, no. 1, 42, 1967.

23. Beddow, J.K.: The Production of Metal Powders by Atomization. Heyden, London, 1978.

24. Dunkley, J.J.: Atomization. *ASM Handbook*, vol. 7, ASM International, Materials Park, OH, 1998.

25. Klar, E.; and Shafer, W.M.: High-Pressure Gas Atomization of Metals. Powder Metallurgy for High Performance Applications. John J. Burke and Volker Weiss, ed., Syracuse University Press, New York, 1972, pp. 57–68.
26. HJE Company, Glens Falls, NY.
27. Tasirin, S.M.: The Effect of Fines on Flow Properties of Binary Mixtures. *Chemical Engineering Communications*. 179, 2000, pp. 101–115.
28. Davies, R.: Size Measurement. *Powder Technology Handbook*, Second ed., Marcel Dekker, Inc., New York, 1997.

TABLE I.—SUMMARY OF FEEDSTOCK PROPERTIES

	Fluoride ($70BaF_2$-$30CaF_2$)		Nichrome (80Ni-20Cr)	Chromia (Cr_2O_3)	Silver (Ag)
	Angular	Spherical			
Fabrication method	Comminution	Gas atomization	Water atomization	Comminution	Gas atomization
Surface morphology	Angular	Spherical	Rounded	Angular	Spherical
Particle size distribution	45 to 106 μm	45 to 106 μm	44 to 74 μm	30 to 44 μm	45 to 100 μm
Theoretical density (g/cm^3)	4.01	4.01	8.57	5.22	10.49
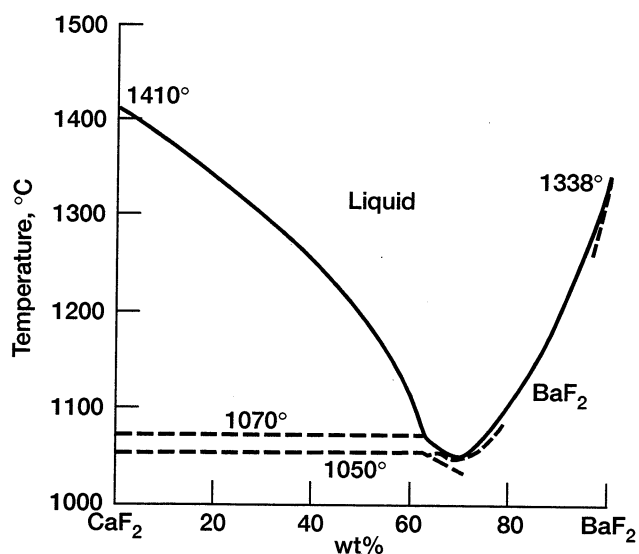
Figure 1.—Binary phase diagram for BaF_2-CaF_2 (ref. 22).

Atmosphere	During melting (A_M)
	In atomizing tank (A_T)
	Temperature (T)
Molten Material	Chemistry (C)
	Viscosity (η)
	Surface tension (γ)
	Melting temperature (T_M)
	Superheat (T_S)
	Density
	Nozzle diameter (D)
Atomizing Fluid	Pressure (P)
	Flow rate
	Velocity
Tank Parameters	Flight path (H)
	Quenching medium (Q)
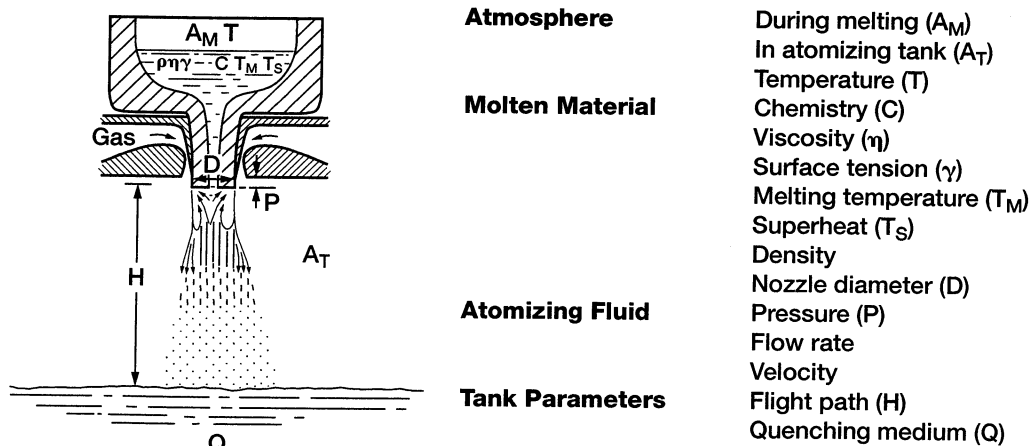
Figure 2.—Main elements of an atomization process (refs. 23 and 24).
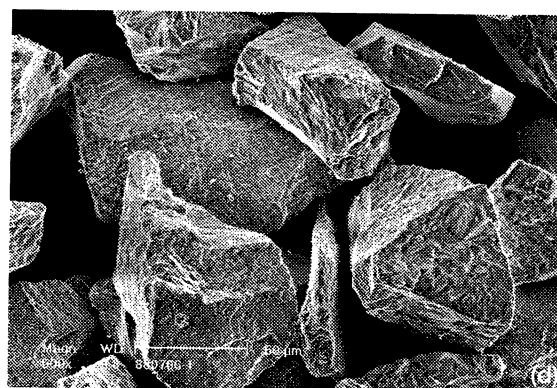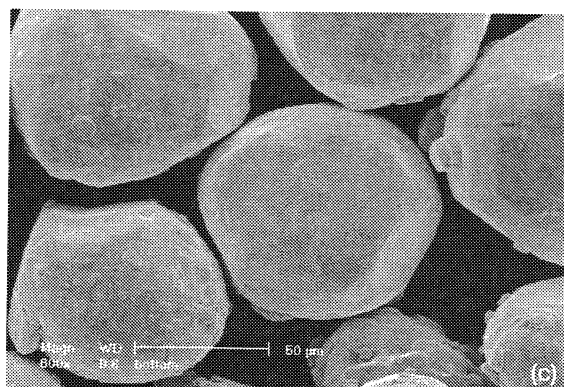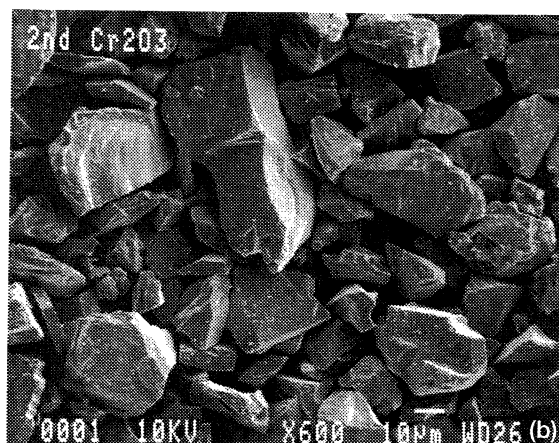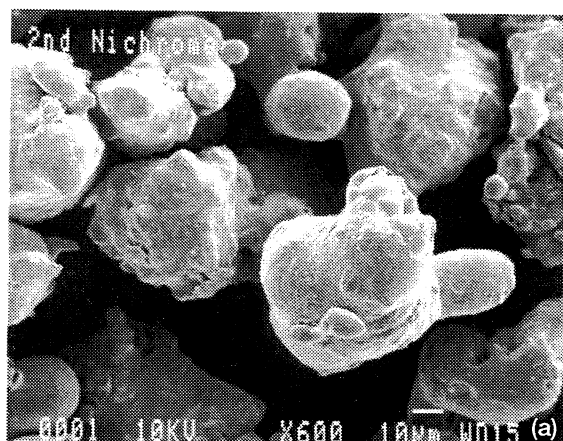
Figure 3.—Representative shapes of the powders in PS304 used in this study (original magnification 600x). (a) Rounded nichrome. (b) Angular chromia. (c) Spherical silver. (d) Angular fluoride.
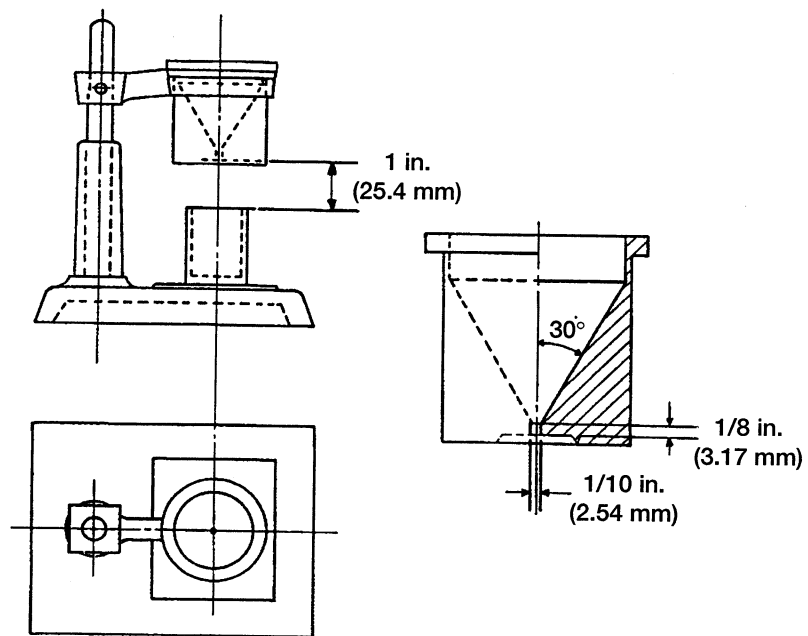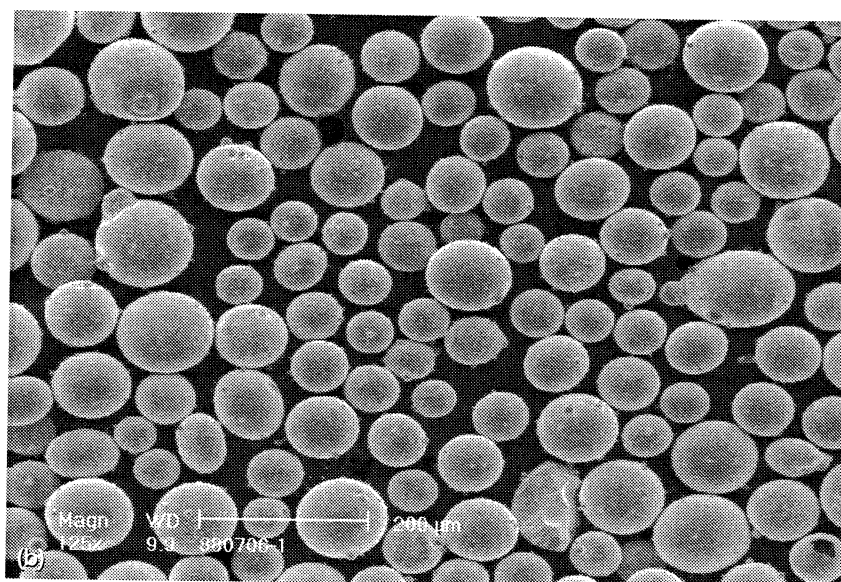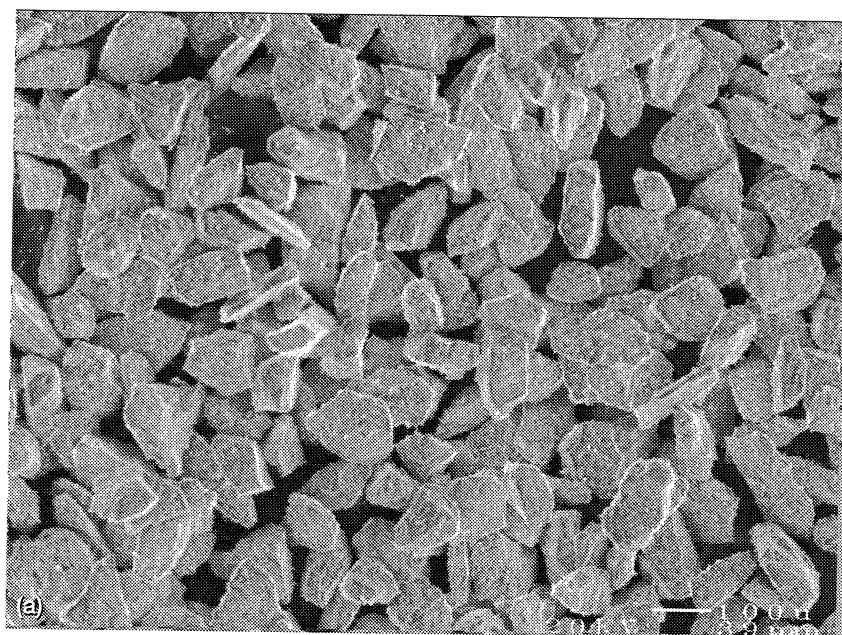
Figure 4.—Flowmeter setup (ref. 23).

Figure 5.—Angular and spherical fluoride powders used in this study
(original magnification 125x). (a) Angular fluoride powder fabricated by
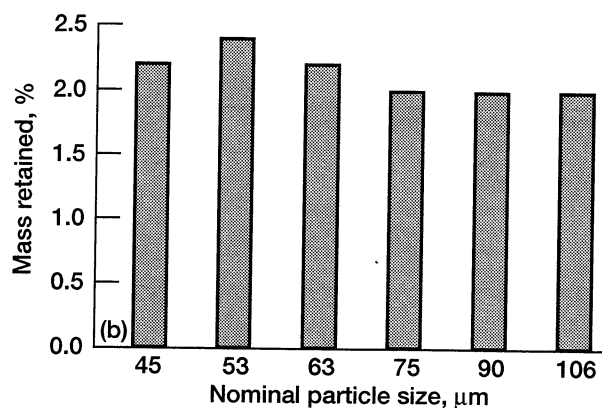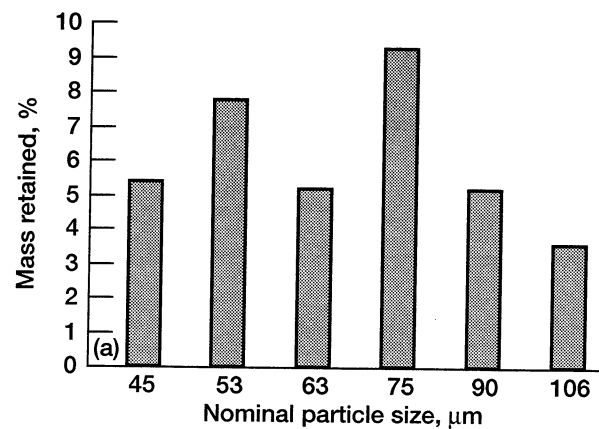comminution. (b) Spherical fluoride powder fabricated by atomization.

Figure 6.—Mass yield of BaF_2-CaF_2 powders from sieving procedure. (a) Comminuted fluorides. (b) Atomized fluorides.

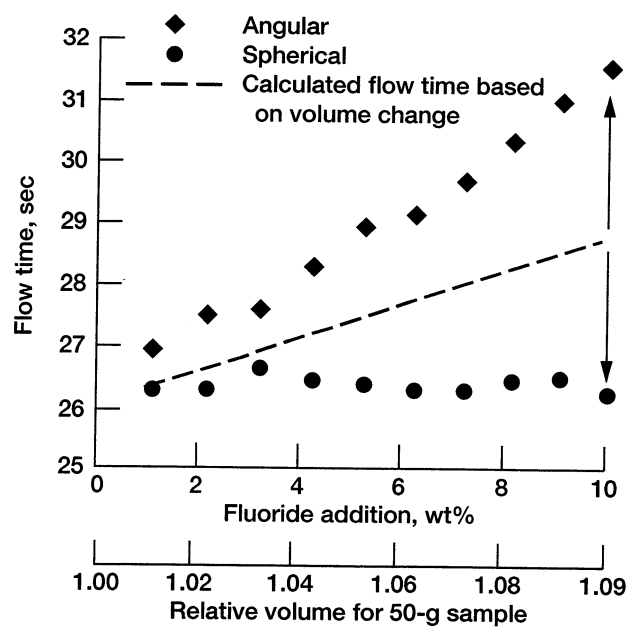Figure 7.—Plot of funnel flow time versus fluoride weight percent.

REPORT DOCUMENTATION PAGE

Public reporting burden for this collection of information is estimated to average 1 hour per response, including the time for reviewing instructions, searching existing data sources, gathering and maintaining the data needed, and completing and reviewing the collection of information. Send comments regarding this burden estimate or any other aspect of this collection of information, including suggestions for reducing this burden, to Washington Headquarters Services, Directorate for Information Operations and Reports, 1215 Jefferson Davis Highway, Suite 1204, Arlington, VA 22202-4302, and to the Office of Management and Budget, Paperwork Reduction Project (0704-0188), Washington, DC 20503.

1. AGENCY USE ONLY (Leave blank)	2. REPORT DATE	3. REPORT TYPE AND DATES COVERED
	January 2002	Technical Memorandum

4. TITLE AND SUBTITLE

Particle Morphology Effects on Flow Characteristics of PS304 Plasma Spray Coating Feedstock Powder Blend

5. FUNDING NUMBERS

WU–708–18–13–00

6. AUTHOR(S)

Malcolm K. Stanford, Christopher DellaCorte, and Daniel Eylon

7. PERFORMING ORGANIZATION NAME(S) AND ADDRESS(ES)

National Aeronautics and Space Administration
John H. Glenn Research Center at Lewis Field
Cleveland, Ohio 44135–3191

8. PERFORMING ORGANIZATION REPORT NUMBER

E–13057

9. SPONSORING/MONITORING AGENCY NAME(S) AND ADDRESS(ES)

National Aeronautics and Space Administration
Washington, DC 20546–0001

10. SPONSORING/MONITORING AGENCY REPORT NUMBER

NASA TM—2002-211206

12a. DISTRIBUTION/AVAILABILITY STATEMENT

Unclassified - Unlimited
Subject Category: 23   Distribution: Nonstandard

Available electronically at http://gltrs.grc.nasa.gov/GLTRS

This publication is available from the NASA Center for AeroSpace Information, 301–621–0390.

12b. DISTRIBUTION CODE

13. ABSTRACT (Maximum 200 words)

The effects of BaF_2-CaF_2 particle morphology on PS304 feedstock powder flow ability have been investigated. BaF_2-CaF_2 eutectic powders were fabricated by comminution (*angular*) and by gas atomization (*spherical*). The fluoride powders were added incrementally to the other powder constituents of the PS304 feedstock: nichrome, chromia, and silver powders. A linear relationship between flow time and concentration of BaF_2-CaF_2 powder was found. Flow of the powder blend with spherical BaF_2-CaF_2 was better than the angular BaF_2-CaF_2. Flow ability of the powder blend with *angular* fluorides decreased linearly with increasing fluoride concentration. Flow of the powder blend with *spherical* fluorides was independent of fluoride concentration. Results suggest that for this material blend, particle morphology plays a significant role in powder blend flow behavior, offering potential methods to improve powder flow ability and enhance the commercial potential. These findings may have applicability to other difficult-to-flow powders such as cohesive ceramics.

14. SUBJECT TERMS

Plasma spray coatings; Solid lubrication; Powder flowability; Powder feedstock; Particle morphology; Coatings; Lubrication; Powders

15. NUMBER OF PAGES

17

16. PRICE CODE

17. SECURITY CLASSIFICATION OF REPORT	18. SECURITY CLASSIFICATION OF THIS PAGE	19. SECURITY CLASSIFICATION OF ABSTRACT	20. LIMITATION OF ABSTRACT
Unclassified	Unclassified	Unclassified	

NSN 7540-01-280-5500

Standard Form 298 (Rev. 2-89)
Prescribed by ANSI Std. Z39-18
298-102